87-1104

A COMPARISON OF NUMERICAL FLUX FORMULAS FOR THE EULER AND NAVIER-STOKES EQUATIONS

Bram van Leer
The University of Michigan
Ann Arbor, Michigan

James L. Thomas
NASA Langley Research Center
Hampton, Virginia

Philip L. Roe
Cranfield Institute of Technology
Cranfield, England

Richard W. Newsome, Major, USAF
Air Force Wright Aeronautical Laboratories
NASA Langley Research Center
Hampton, Virginia

Summary

Numerical flux formulas for the convection terms in the Euler or Navier-Stokes equations are analyzed with regard to their accuracy in representing steady nonlinear and linear waves (shocks and entropy/shear waves, respectively). Numerical results are obtained for a one-dimensional conical Navier-Stokes flow including both a shock and a boundary layer. Analysis and experiments indicate that for an accurate representation of both layers the flux formula must include information about all different waves by which neighboring cells interact, as in Roe's flux-difference splitting. In comparison, Van Leer's flux-vector splitting, which ignores the linear waves, badly diffuses the boundary layer. The results of MacCormack's scheme, if properly tuned, are significantly better. The use of a sufficiently detailed flux formula appears to reduce the number of cells required to resolve a boundary layer by a factor 1/2 to 1/4 and thus pays off.

1. Introduction

In finite-volume codes for the Euler and Navier-Stokes equations a central place is taken by the algorithm that accounts for the inviscid interaction of adjacent fluid cells at their interface. Such an algorithm combines two distinct sets of state quantities, representing the states on both sides of the interface, into one set of fluxes normal to the interface.[1]

Physically speaking there is only one correct value for the flux vector. To find it we must solve the Riemann problem governed by the one-dimensional inviscid flow equations

$$u_t + f(u)_x = 0 \qquad (1)$$

(x measuring distance to the interface) for the initial values

$$u = \begin{cases} u_L & x < 0 \ , \\ u_R & x > 0 \ , \end{cases} \qquad (2)$$

where u_L and u_R are the left and right interface states. If $U(x/t; u_L, u_R)$ denotes the self-similar solution to this problem, the interface flux reads

$$f(u_L, u_R) = f(U(0; u_L, u_R)) \qquad (3)$$

This is Godunov's[2] flux formula.

From a numerical point of view, though, it seems wasteful to exactly solve the Riemann problem at every interface (the solution procedure is iterative); an approximate solution, tuned to the overall accuracy of the discretization, should do. In this paper we investigate how good the approximation needs to be, in particular when incorporated in a Navier-Stokes code.

The simplest recipe for a numerical flux $f(u_L,u_R)$ is to average the fluxes corresponding to u_L and u_R:

$$f(u_L,u_R) = \frac{1}{2}\{f(u_L) + f(u_R)\} \ . \qquad (4)$$

In the final update this leads to central differencing, which is inherently unstable: it decouples adjacent cells. We may use the numerical difference between the states, i.e., $u_R - u_L$, to couple the cells; this amounts to adding artificial dissipation to the flux. The freeedom in choosing a numerical flux essentially is the freedom in selecting the matrix coefficient $Q(u_L,u_R)$ of the dissipation term:[1]

$$f(u_L,u_R) = \frac{1}{2}\{f(u_L) + f(u_R)\} - \frac{1}{2} Q(u_L,u_R) \cdot (u_R - u_L). \qquad (5)$$

In the next section we analyze and compare several representative flux formulas developed for Euler codes, including some that cannot be written in the form (5). In the remaining sections we test their performance in a discriminating Navier-Stokes problem and summarize the results.

2. Dissipative Properties of Inviscid Flux Formulas

Roe

Roe's[3] numerical flux is based on the solution of Riemann's problem with initial values (2) for the linearized equation

$$u_t + A(u_L,u_R)\, u_x = 0 \ . \qquad (6)$$

Here $A(u_L,u_R)$ is a mean value of the Jacobian $A(u)$ of $f(u)$ with properties

(i) $A(u,u) = A(u)$; (7)

(ii) $A(u_L,u_R)$ has a complete set of real eigenvalues and eigenvectors ; (8)

(iii) $A(u_L,u_R) \cdot (u_R - u_L) = f(u_R) - f(u_L)$. (9)

Property (i) ensures that the approximate solution tends to the exact solution for small data; property (iii) ensures that the approximate solution is exact if u_L and u_R can be connected by a single discontinuity parallel to the interface, no matter how large. This follows upon comparing (9) with the jump equation

$$V(u_R - u_L) = f(u_R) - f(u_L) \ . \qquad (10)$$

Clearly, $u_R - u_L$ is an eigenvector of $A(u_L,u_R)$ and V, the discontinuity's speed, is the corresponding eigenvalue.

The numerical flux based on this "approximate Riemann solver" reads

$$f(u_L, u_R) = \frac{1}{2}\{f(u_L) + f(u_R)\} - \frac{1}{2}|A(u_L,u_R)| \cdot (u_R - u_L) ; \quad (11)$$

$|A|$ denotes the matrix with the same eigenvectors as **A,** whose eigenvalues are the absolute values of the eigenvalues $\{a^{(k)}\}$ of **A.** (The latter represent the characteristic speeds normal to the interface.)

A consequence of (9) is: if an eigenvalue of $A(u_L,u_R)$ vanishes, the corresponding eigenvalue of the dissipation matrix vanishes too. This leads to a crisp representation -- with at most one interior state -- of steady shocks and contact discontinuities, if aligned with an interface (and expansion shocks, ignored here).

Osher

Another approximate Riemann solver, with similar properties, is due to Osher;[4] it leads to the flux formula

$$f(u_L,u_R) = \frac{1}{2}\{f(u_L) + f(u_R)\} - \frac{1}{2}\int_{u_L}^{u_R} |A(u)|\, du \ , \quad (12)$$

where the integral is carried out along a path piecewise parallel to the eigenvectors of $A(u)$. The differentiability of this flux has the consequence that steady shocks are represented with one to two interior states rather than zero to one interior state, as with Roe's flux.

Harten-Lax/Roe

Harten and Lax[5] observed that it is not necessary to account for all characteristic waves separately in the numerical flux. They introduced an amplitude-square weighted wave speed $V(u_L,u_R)$:

$$V(u_L,u_R) = \frac{(w(u_R) - w(u_L)) \cdot (f(u_R - f(u_L))}{(w(u_R) - w(u_L)) \cdot (u_R - u_L)} \ , \quad (13)$$

here $w(u)$ is the gradient of an entropy function associated with Eq. (1). If u_L and u_R can be connected by a single discontinuity, $V(u_L,u_R)$ equals the speed of that discontinuity, as follows from (10).

The approximate Riemann solution of Harten and Lax incorporates three wave speeds and has little advantage over Roe's. It has been suggested by **Roe,** [6], however, to replace the entire dissipation matrix $Q(u_L,u_R)$ by a scalar **like** $|V(u_L,u_R)|$:

$$f(u_L,u_R) = \frac{1}{2}(f(u_L) + f(u_R)) - \frac{1}{2}|V(u_L,u_R)| \cdot (u_R - u_L) \ . \quad (14)$$

This formula again leads to the representation of steady discontinuities with minimal spread, while requiring less computational effort than (11).

This exhausts the collection of flux formulas that recognize all different characteristic waves and yield zero dissipation when these waves are steady.

Van Leer

4 compromise already **is** Van Leer's differentiable flux-split formula, designed to make the dissipation vanish only in steady shocks. Flux splitting is writing $f(u)$ as the sum of a forward **flux** $f^+(u)$ and a backward flux $f^-(u)$,

$$f(u) = f^+(u) + f^-(u) \ , \quad (15)$$

with

$$df^+(u)/du \equiv B^+(u) \geq 0 \ , \quad (16)$$

$$df^-(u)/du \equiv B^-(u) \leq 0 \ . \quad (17)$$

The corresponding numerical flux formula reads

$$f(u_L,u_R) = f^+(u_L) + f^-(u_R) \ ; \quad (18)$$

we may rewrite this as

$$f(u_L,u_R) = \frac{1}{2}\,(f(u_L) + f(u_R)) - \frac{1}{2}\int_{u_L}^{u_R} |B(u)|\, du \ , \quad (19)$$

with

$$|B(u)| \equiv B^+(u) - B^-(u) \ , \quad (20)$$

to make it look like Osher's formula (12). Although the integration in (19) is independent of the path, since $|B(u)|$ **is** a perfect gradient, it is useful to imagine a path along which the Mach number (based on the normal flow velocity) varies monotonically. If u_L and u_R form a steady shock, one eigenvalue of $|B(u)|$ vanishes somewhere in between; **just** as for Osher's formula, we find steady shock structures with one *to* two interior states.

If, however u_L and u_R form a steady contact discontinuity, with or without slip, $|B(u)|$ has no vanishing eigenvalue anywhere along the path. This leads to the numerical diffusion of such a discontinuity, stopped only by nonlinear effects in the flow region in which it is embedded.

Steger-Warming

Even worse is the splitting of Steger and Warming,[8] corresponding to the numerical flux function

$$f(u_L,u_R) = \frac{1}{2}(f(u_L)+f(u_R)) - \frac{1}{2}(|A(u_R)| \cdot u_R - |A(u_L)| \cdot u_L) \ . \quad (21)$$

In spite of the appearance of $|A(u)|$ in this formula, it does not lead *to* vanishing dissipation in any steady wave. The dissipation matrix to be considered is

$$\frac{d(|A(u)| \cdot u)}{du} = |A(u)| + u^T \frac{d|A(u)|}{du} \ , \quad (22)$$

the eigenvalues of which are discontinuous whenever the corresponding eigenvalues of $A(u)$ vanish.

Rusanov/Davis/Yee

Even further down the line are the numerical fluxes used by Davis[9] and Yee[10], in which $Q(u_L,u_R)$ is a scalar with a value tuned to the spectral radius of $A(u_L,u_R)$, e.g.,

$$f(u_L,u_R) = \frac{1}{2}(f(u_L) + f(u_R)) - \frac{1}{2}\max_k |a^{(k)}(u_L,u_R)| \cdot (u_R - u_L), \quad (23)$$

regardless of the relative strengths of the characteristic waves. This formula is actually due to Rusanov.[11]

The dissipation coefficient in **(23)** does not vanish in any steady discontinuity and must be considered too large for steady flow. **A** factor $C < 1$ may be introduced to enable the user to deliberately reduce the dissipation level:

$$f(u_L,u_R) = \frac{1}{2}(f(u_L) + f(u_R)) - \frac{C}{2}\max_k |a^{(k)}(u_L,u_R)| \cdot (u_R - u_L). \quad (24)$$

This, of course, will make the quality of the results subject *to* trial and error.

Jameson-Schmidt-Turkel

The flux formula of Jameson et al.,[12] although not written in terms of interface values, is related to **(24)** and treats steady discontinuities correspondingly. For the flux at the interface between cells i and i + 1 we may write, with minor adjustments,

$$f_{i+1/2} = f\left(\frac{u_i + u_{i+1}}{2}\right) + \frac{C}{8} \max_k |a^{(k)}\left(\frac{u_i + u_{i+1}}{2}\right)| \, \Delta^3_{i+1/2} u \, . \quad (25)$$

In part this is consistent with

$$u_L = u_i + \frac{1}{2}(u_{i+1} - u_i) = \frac{1}{2}(u_i + u_{i+1}) \, , \quad (26a)$$

$$u_R = u_{i+1} - \frac{1}{2}(u_{i+1} - u_i) = \frac{1}{2}(u_i + u_{i+1}) \, , \quad (26b)$$

in part with

$$u_L = u_i + \frac{1}{4}(u_{i+1} - u_{i-1}) \, , \quad (27a)$$

$$u_R = u_{i+1} - \frac{1}{4}(u_{i+2} - u_i) \, ; \quad (27b)$$

the coefficient C again is user-specified. This flux, however, is not fully satisfactory; an extra dissipation term must be added to suppress numerical oscillations near discontinuities. In the schemes discussed before, such a term does not enter the flux formula; instead, non-oscillatory interpolation is used to compute interface values from the discrete solution.

MacCormack

Consider, finally, the flux formula of the most popular finite-difference scheme, viz. MacCormack's[13] explicit method. This basically is a second-order time-accurate scheme; a one-dimensional variant of the scheme includes the flux

$$f_{i+1/2} = \frac{1}{2}(f(\tilde{u}_i) + f(u_{i+1})) \, , \quad (28a)$$

with

$$\tilde{u}_i = u_i - \frac{\Delta t}{\Delta x}(f(u_{i+1}) - f(u_i)) \, . \quad (28b)$$

Molding this in the form **(5)** we get

$$f_{i+1/2} \equiv f(u_i, u_{i+1}) = \frac{1}{2}(f(u_i) + f(u_{i+1}))$$

$$- \frac{1}{2}\frac{\Delta t}{\Delta x} A(u_i, \tilde{u}_i) A(u_i, u_{i+1}) \cdot (u_{i+1} - u_i) \, ; \quad (29)$$

for steady-state calculations one often uses the maximum time-step locally allowed, i.e.,

$$(\Delta t)_i = \frac{\Delta x}{\max_k |a_i^{(k)}|} \, , \quad (30)$$

yielding

$$f(u_i, u_{i+1}) = \frac{1}{2}(f(u_i) + f(u_{i+1}))$$

$$- \frac{1}{2}\frac{A(u_i, \tilde{u}_i)}{\max_k |a_i^{(k)}|} A(u_i, u_{i+1}) \cdot (u_{i+1} - u_i) \, . \quad (31)$$

This formula lacks dissipation: if some characteristic speed vanishes near $x = x_i$, the corresponding eigenvalue of the dissipation matrix vanishes quadratically, as the latter contains two factors $(A(u_i) + O(\Delta x))$. This is known to lead to nonlinear instabilities;[14] in practice an extra dissipation term is added with a scalar coefficient proportional to the second pressure difference (the same term is used for Jameson's flux). Such a term in particular increases the dissipation at the foot and the head of a shock, thus suppressing numerical oscillations; a contact discontnuity, across which the pressure is constant, is not affected.

3. Testing in a Navier-Stokes code

Practical comparisons of different flux formulas have been made by some of the authors cited above[7,9,10] and (among others) by Anderson et al.,[15] but are mostly limited to Euler applications and the aspect of shock resolution. It appears that even formulas (24) and (25), with C properly trimmed, yield acceptable profiles for steady grid-aligned shocks, with three internal cells, The quality of numerical representations of slip/contact surfaces may deteriorates more strongly because in these linear discontinuities there is no intrinsic steepening mechanism counteracting the numerical diffusion. The Euler solutions considered, however, were not discriminating in this respect.

This situation changes drastically once Navier-Stokes solutions are sought: attached boundary layers must now be resolved where the perfect-slip consideration used to be applied. To study the interference of numerical dissipation with the modeling of physical dissipation, we conducted a series of numerical experiments using different formulas for the inviscid fluxes in the same carrier code. This implicit code has been described previously[16] and is set up to compute two- or three-dimensional viscous or inviscid flows over conical bodies. Assuming conical flow reduces the computation to two dimensions; for a circular cone at zero angle of attack the solutions become one-dimensional, varying only with the angle 8 between streamline and cone surface. All pertinent conclusions can be drawn from the one-dimensional conical-flow results, a selection of which is shown in the figures below.

Figure 1 is the most discriminating, comparing solutions of fit-order accuracy (i.e., with interface values based on uniform distributions in the cells) on a sequence of grids. The numerical fluxes are based on Van Leer's[7] flux-vector splitting (FVS, left) and Roe's[3] flux-difference splitting (FDS, right), respectively. Plotted is the dimensionless temperature T/T_∞ as a function of 8; because of the adiabatic-wall condition the difference scheme has to provide the proper wall temperature, which in this case (10° cone, $M_\infty = 7.95$, $Re = 0.42 \times 10^6$, Pr = 0.72) equals about 11.72. With Roe's fluxes the solution has essentially converged on the coarsest grid (18 cells) whereas van Leer's fluxes considerably broaden the boundary layer and leave a significant error in the wall temperature even on the 74-cell grid The difference in performance can entirely be attributed to a difference in the numerical coefficients of conduction and shear viscosity. In the case of FDS these are negligible because the normal velocity component is negligible in the boundary layer: in the case of FVS they remain finite, scaling with the sound speed. Furthermore, the FVS shock is broader than the FDS shock, as expected.

* The converged solutions *are* limited in accuracy by the discretization of the redundant coordinate, which is the **same** for all **6 grids.**

The solution obtained with the FDS scheme is so accurate that one might be tempted to use this scheme for computing two- and three-dimensional solutions. It must be remembered, however, that the scheme after all is only first-order accurate: it will give evidence of its high dissipative power in any direction for which the flow-velocity component differs enough from zero.

Figure 2 shows the effect of using a higher-order interpolation to obtain interface values; the results here are for the fully one-sided second-order scheme (denoted by $\kappa = -1$, see Anderson et al.[15]). For FDS (not shown) there is no further benefit, but for FVS there is a clear improvement in the representation of the boundary layer: on the finest grid the correct wall tempeature is reached. Moreover, the shock representation now rivals that of the FDS scheme.

Figure 3 shows results obtained with a different code,[16] based on the explicit MacCormack scheme with local time-step values. As expected, the shock is significantly wider than in Figures 1 and 2, but the accuracy in the boundary layer is better than for FVS, with near-convergence to the proper wall temperature on the medium-fine grid.

Figure 4 shows a blow-up of the boundary layer, with the results for the 37-cell grid taken from Figures 2 and 3, and two more solutions obtained on the same grid with quadratically interpolated interface values ($k = 1/3$, a third-order scheme) and FVS or FDS. The most accurate FVS results are still not as good as the MacCormack results (at least, in the boundary layer).

Finally, Figures 5 and 6 show results of the best performing methods on the 37-cell grid, for the flow velocity (normalized by c_∞) and the pressure (normalized by p_∞).

4. Conclusions

The analysis and numerical results presented above indicate that for an accurate representation of both grid-aligned shocks and boundary layers in steady Navier-Stokes solutions, on all but the finest grids, the numerical flux formula for the convective terms must include information about all different waves by which neighboring cells interact. Examples of such formulas are Roe's and Osher's. When tested in a computation of one-dimensional conical flow, the results obtained with Roe's flux-difference splitting, based on the full Riemann solution, are far more accurate than those of van Leer's flux-vector splitting, which ignores entropy and shear waves.

The performance of MacCormacks scheme in the boundary layer is better than that of any of the flux-vector split schemes tested, even the third-order scheme, but is inferior in shock rendition. It can not stand comparison to any of the flux-difference split schemes incorporating Roe's flux formula, regardless of the order of accuracy. MacCormacks scheme appears to require at least twice as many cells in the boundary layer as Roe's formula, and Van Leer's formula at least four times as many.

There is no hope for flux formulas of the Rusanov or Jameson type. With careful trimming of the user-specified dissipation coefficient these will at best compete with the flux-split formula. Just as the latter, they are best suited for Euler codes and restricted to applications in which contact/slip surfaces lie outside the region of interest.

An interesting flux formula that remains to be tested is the one based on Harten and Lax's dominant-wave speed; this promises Roe-like results at significant computational savings.

References

1. B. van Leer, Lectures in Applied Mathematics 22 (1985), part 2, pp. 327-336.
2. S.K. Godunov, Mat. Sb. 47 (1959), pp. 271-306.
3. P.L. Roe, Lecture Notes in Physics 141 (1980), pp. 354-359.
4. S. Osher, North Holland Math. Studies 47 (1981), pp. 179-205.
5. A. Harten and P.D. Lax, SIAM J. Numer. Anal. 18 (1981), pp. 289-315.
6. P.L. Roe, ICASE Report 84-53 (1984).
7. B. van Leer, Lecture Notes in Physics 170 (1982), pp. 507-512.
8. J. Steger and R.F. Warming, J. Comp. Phys. 40 (1981), pp. 263-293.
9. S.F. Davis, ICASE Report 84-20 (1984).
10. H. Yee, "Construction of explicit and implicit symmetric TVD schemes and their applications," J. Comp. Phys. 68 (1987), pp. 151-179.
11. V.V. Rusanov, Zh. Vych. Matem. Mat. Fiz 1(2) (1961), pp. 267-279.
12. A. Jameson, W. Schmidt and E. Turkel, AIAA Paper 81-1259 (1981).
13. R.W. MacCormack, AIAA Paper 69-354 (1969).
14. S.Z. Burstein, J. Comp. Phys. 1 (1966), pp. 198-222.
15. W.K. Anderson, J.L. Thomas and B. van Leer, AIAA J. 24 (1986), pp. 1453-1460.
16. R.W. Newsome, AIAA Paper 85-0111 (1985).

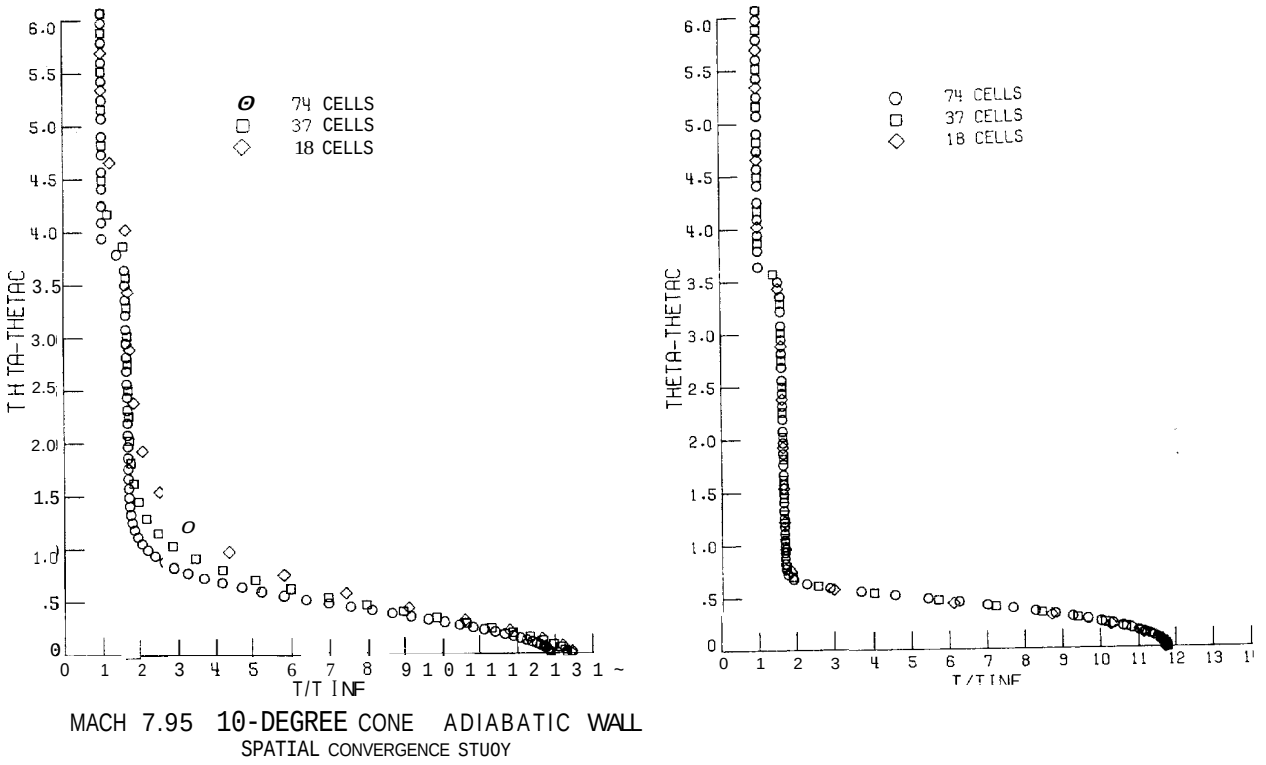

Fig. 1. Comparison of first-order-accurate solutions obtained with Van Leer's flux-vector splitting (FVS, left) and Roe's flux-difference splitting (FDS, right), for hypersonic cone flow.

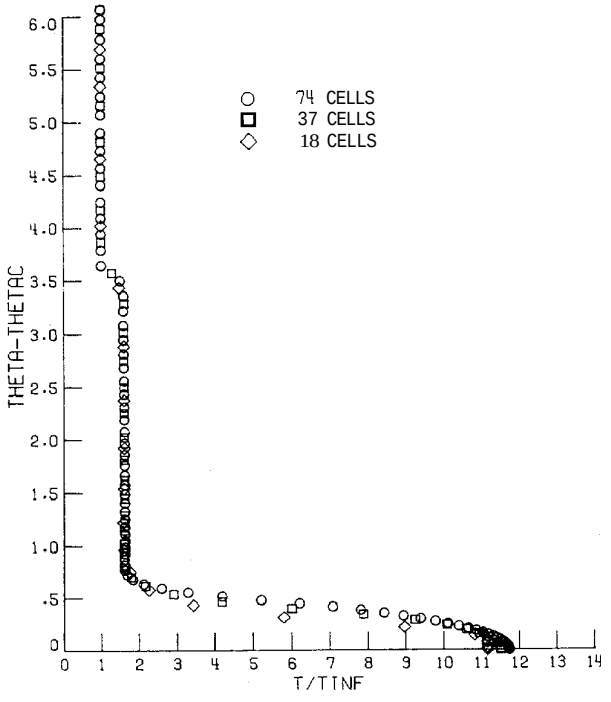

Fig. 2. Second-order-accurate solutions (k = -1) obtained with FVS.

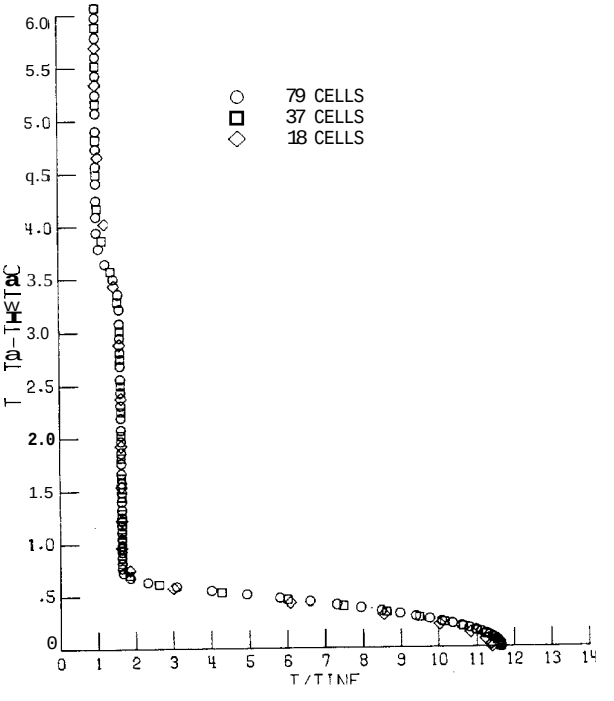

Fig. 3. Second-qrder accurate solutions obtained with MacCormack's method.

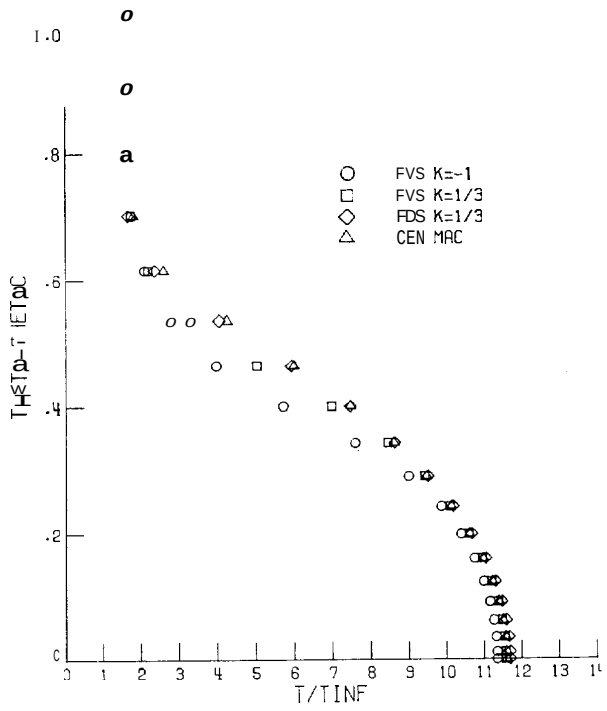

MACH 7.95 10-DEGREE CONE ADIABATIC WALL
SPATIAL CONVERGENCE STUDY

Fig. 4. Comparison of boundary-layer solutions on the 37-cell grid. For k = 1/3 the FVS and FDS solution are third-order accurate in smooth regions.

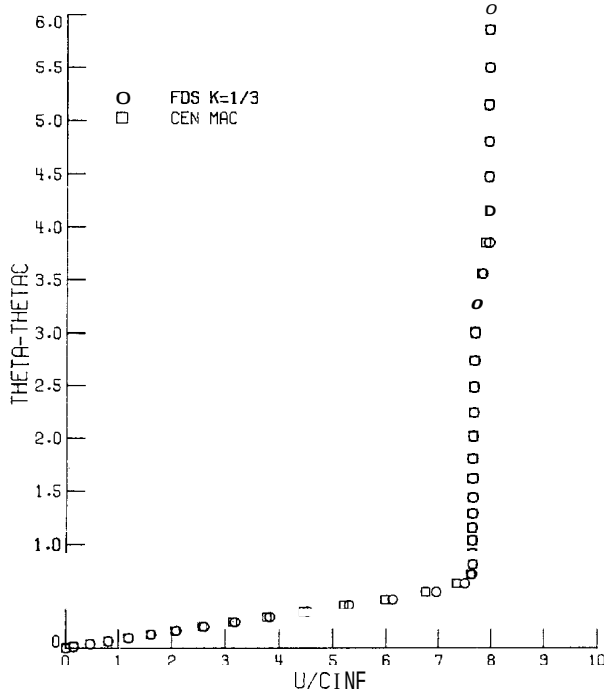

Fig. 5. Solutions obtained with the best-performing schemes on the 37-cell grid: velocity plot.

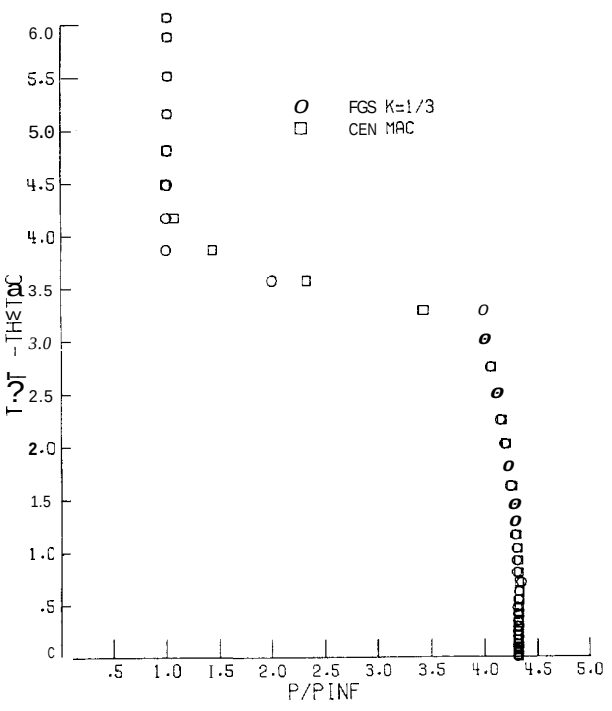

Fig. 6. Solutions obtained with the best-performing schemes on the 37-cell grid: pressure plot.